SUPPLEMENTAL DATA

Supplemental Figures

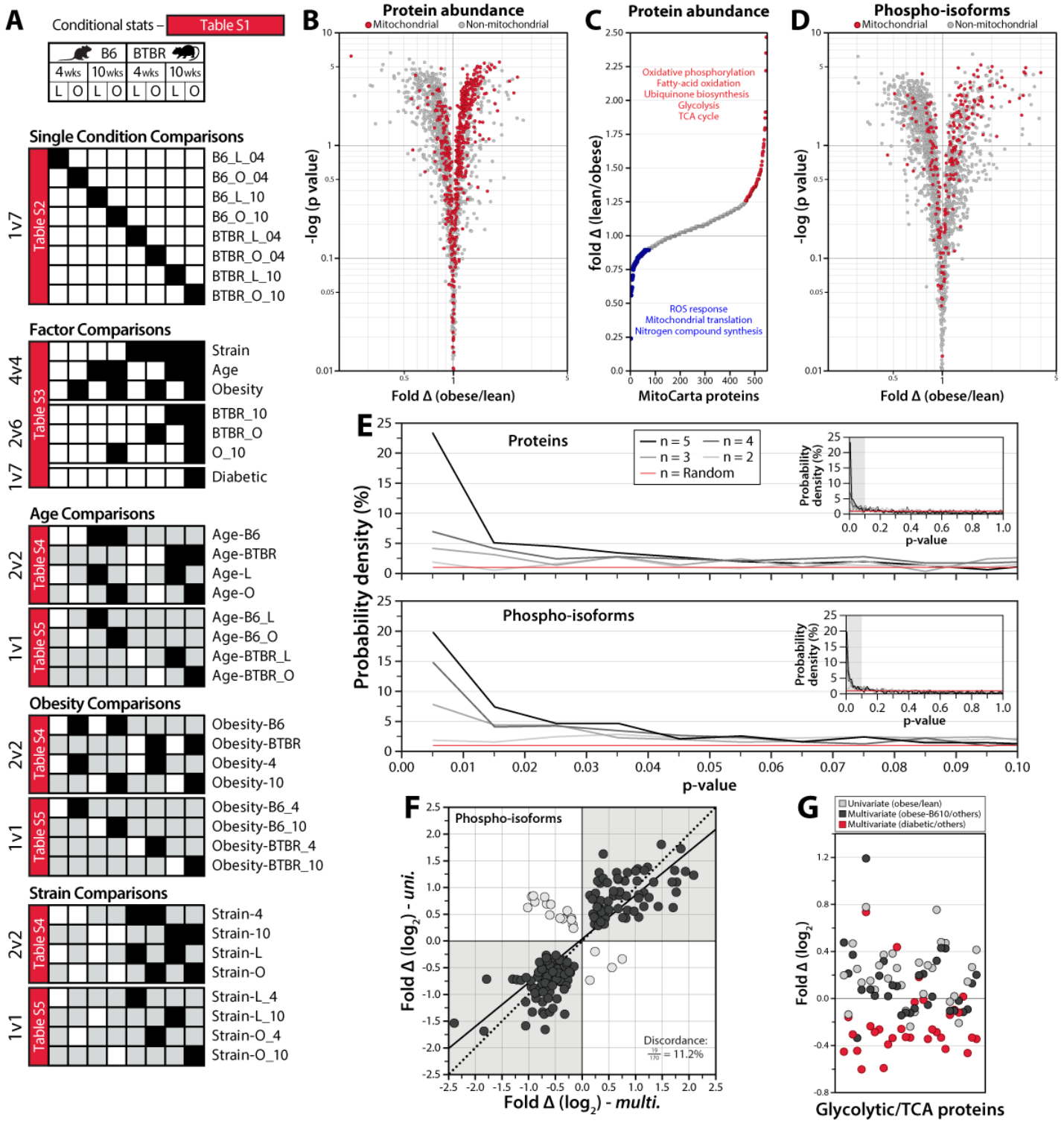

Figure S1. Data analysis for the univariate and multivariate studies, Related to Figure 1. A) Visual key depicting all mouse sample comparisons contained in Tables S1-5. For relative fold-change comparisons made for each proteomic/phosphoproteomic measurement, the cells in the grid below the header of metabolic conditions indicate which samples were used for calculating the numerator (highlighted in black) or denominator (highlighted in white). Samples highlighted in grey were not utilized for the given comparison. The names of the Supplementary Tables (Tables S1-5) containing the statistical analysis for each comparison are indicated (red highlighting). B) Volcano plot of fold protein abundance change (obese/lean) vs. -log (p value) for each mitochondrial (red) and non-mitochondrial (grey) protein measured (univariate). C) Mitochondrial proteins rank ordered (x-axis) and graphed by fold change (y-axis). Analysis of significant changes (q<0.1) for mitochondrial proteins in *panel B* revealed modifications in the indicated mitochondrial pathways (increasing shown in red, decreasing shown in blue). D) Volcano plot of non-normalized protein phosphorylation changes, as in *panel B* for protein changes

(univariate). E) Distribution of p-values (from 0 to 0.1) based on the number of replicate measurements comparing lean and obese 10 week-old B6 mice (multivariate), for both proteins (top) and phosphoisoforms (bottom). Lines connect the average probability densities (% of measurements falling into each bin) of p-values (100 bins of width 0.01), with the inset showing the entire range of p-values (from 0 to 1.0). The red line at a probability density of 1% indicates the distribution of theoretically random p-values. F) Abundance fold-change (obese/lean) for all phosphoisoforms with significant obesity-dependent alterations (q<0.1) between 10 week-old lean and obese B6 mice in both experiments (multivariate on the x-axis and univariate on the y-axis). The percent of measurements in discordance between the two studies (light grey circles) is indicated. G) Abundance fold changes for individual glycolytic and TCA cycle proteins (see Table S2) in the univariate experiment (obese/lean in light grey) and the multivariate experiment (obese 10-week B6 relative to all other conditions in black, obese 10-week BTBR relative to all other conditions in red).

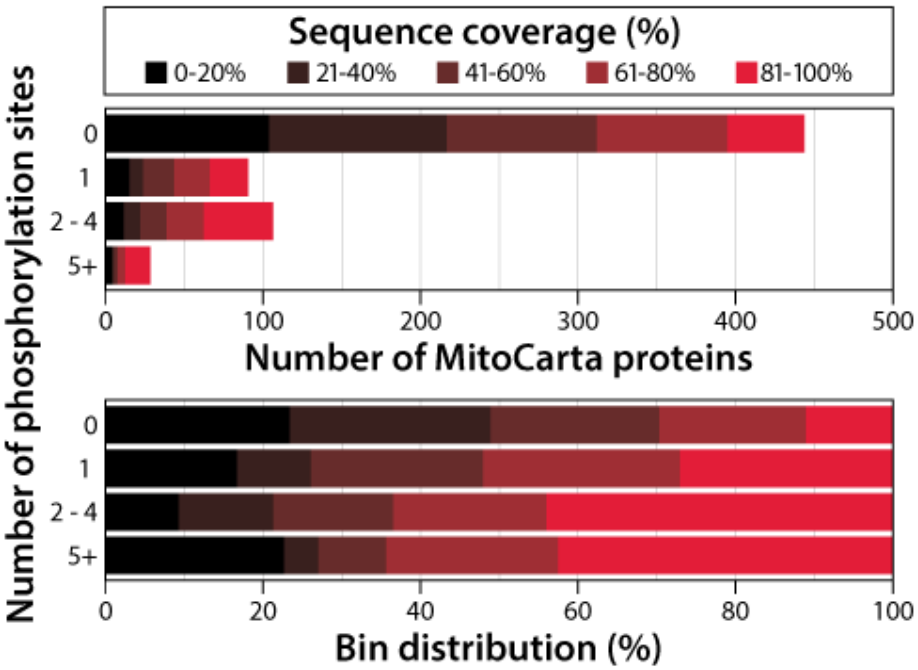

Figure S2. Phosphorylation of mitochondrial proteins across various expression levels, Related to Figure 2. All mitochondrial proteins (MitoCarta) are binned based on the number of phosphorylation sites detected (0, 1, 2-4, 5+). Distributions of sequence coverage, as a proxy for absolute abundance rank, are indicated by color (top). The percent distribution of sequence coverage is plotted against the number of phosphorylation sites (bottom).

A

Protein Kinase	Sequence Preference	MitoCarta Phospho-sites	MitoCarta Phospho-proteins	Total Phospho-sites	Total Phospho-proteins
PKA	R-X-s/t R-R/K-X-s/t K-R-X-X-s/t	101	75	1858	1334
CK1	S-X-X-s/t S/T-X-X-X-s	184	111	3725	2038
CK2	s/t-X-X-E	93	76	1399	1069
GSK3	s-X-X-X-S	111	75	2327	1391
CDK2	s/t-P-X-K/R	20	20	710	590
CAMK2	R-X-X-s/t R-X-X-s/t-V	126	97	2880	1851
ERK/MAPK	P-X-s/t-P V-X-s/t-P P-E-s/t-P	35	34	926	745
PKB/AKT	R-R/S/T-X-s/t-X-S/T R-X-R-X-X-s/t	29	27	680	569
PKC	R-X-X-s/t-X-R	1	1	90	84
PKD	L/V/I-X-R/K-X-X-s/t	39	36	967	730
LCK	I/E/V-y-E/G-E/D/P/N-I/V/L	0	0	2	2
ABL	I/V/L-y-X-X-P/F	0	0	8	8
SRC	E/D-X-X-y-X-X-D/E/A/G/S/T	2	2	12	12
ALK	y-X-X-I/L/V/M	5	5	42	41
EGFR	D/P/S/A/E/N-X-y-V/L/D/E/I/N/P	5	5	37	35
CDK1	s/t-P-X-K/R s/t-P-K/R	34	30	1093	827
AURORA	R/K-X-s/t-I/L/V	16	15	409	376
AURORA-A	R/K/N-R-X-s/t-M/L/V/I	4	4	197	180
PLK	D/E-X-s/t-V/I/L/M-X-D/E	6	5	43	42
PLK1	E/D-X-s/t-F/L/I/Y/W/V/M	33	27	221	206
NEK6	L-X-X-s/t	43	37	594	498
CHK1/2	L-X-R-X-X-s/t	12	12	440	350
CHK1	M/I/L/V-X-R/K-X-X-s/t	45	41	1191	896
PDK1	F-X-X-F-s/t-F/Y	0	0	8	8
NIMA	F/L/M-R/K-R/K-s/t	1	1	25	25

Figure S3. Phosphorylation motif analysis, Related to Figure 5. A) All kinases and known substrate consensus sequences from the PHOSIDA database are indicated, with X indicating any amino acid and a red lower-case letter indicating the phosphorylated residue. The number of mitochondrial (MitoCarta) and total (MitoCarta and non-MitoCarta) phosphorylation sites and phosphoproteins identified by MS/MS are listed that satisfy the consensus sequence requirements for each kinase. B) All motifs identified by Motif-X analysis of our entire phosphoproteomic dataset (group by the polarity of fixed residues) and those specific to MitoCarta proteins.

B

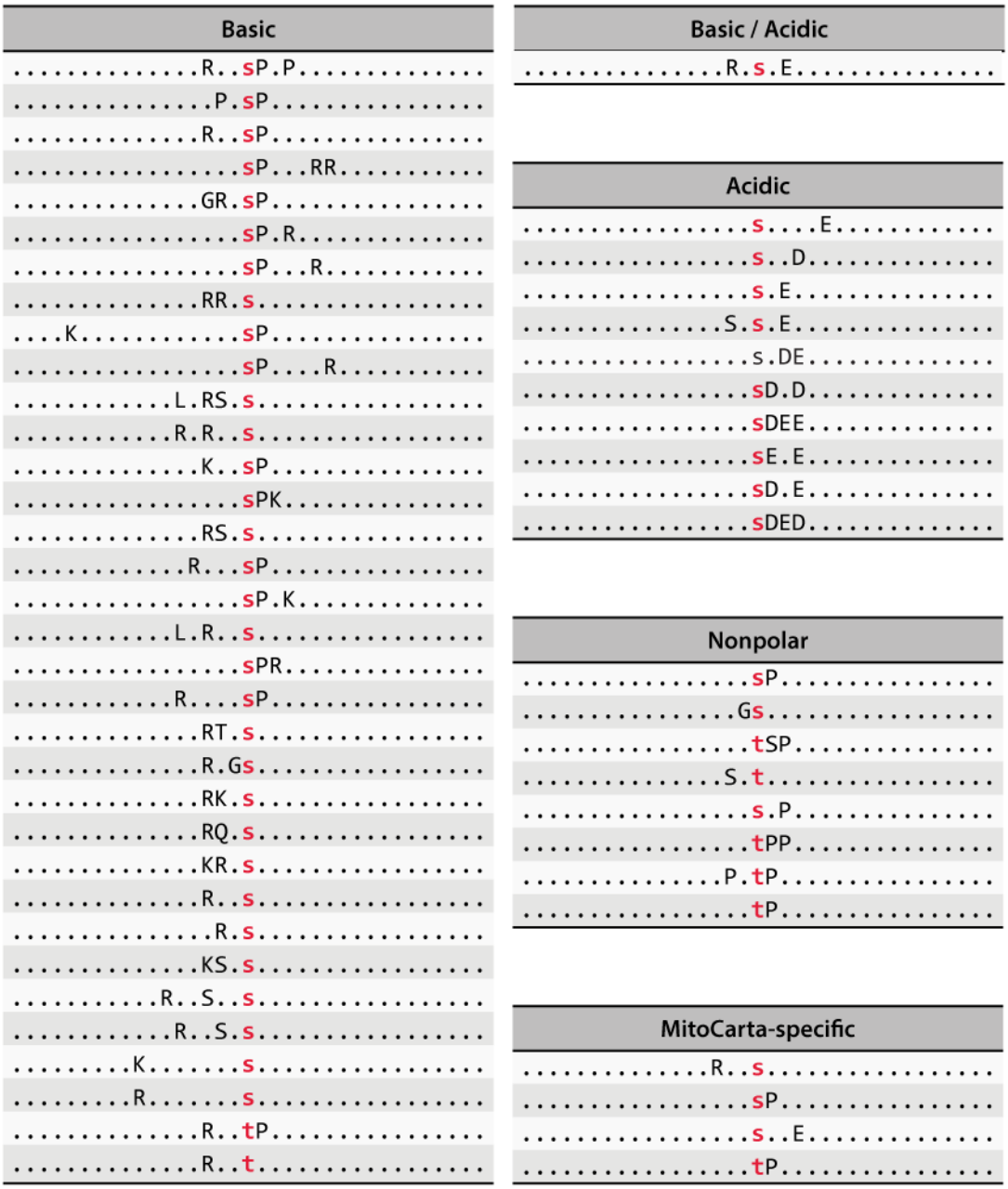

Figure S3 (Continued).

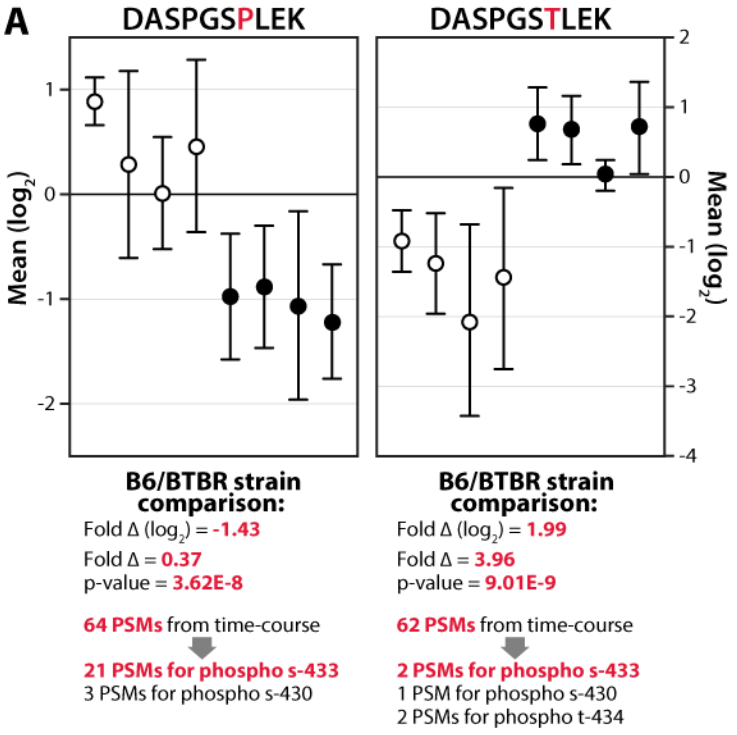

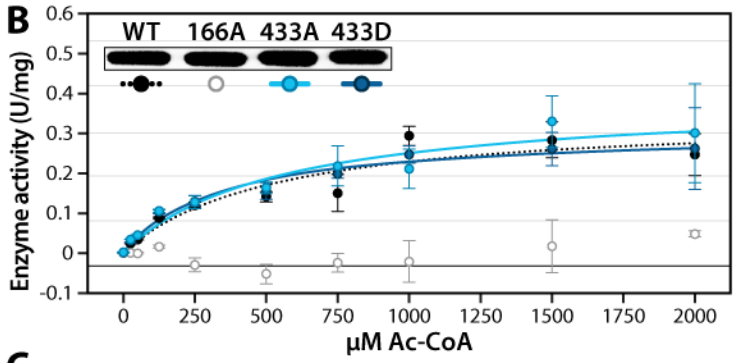

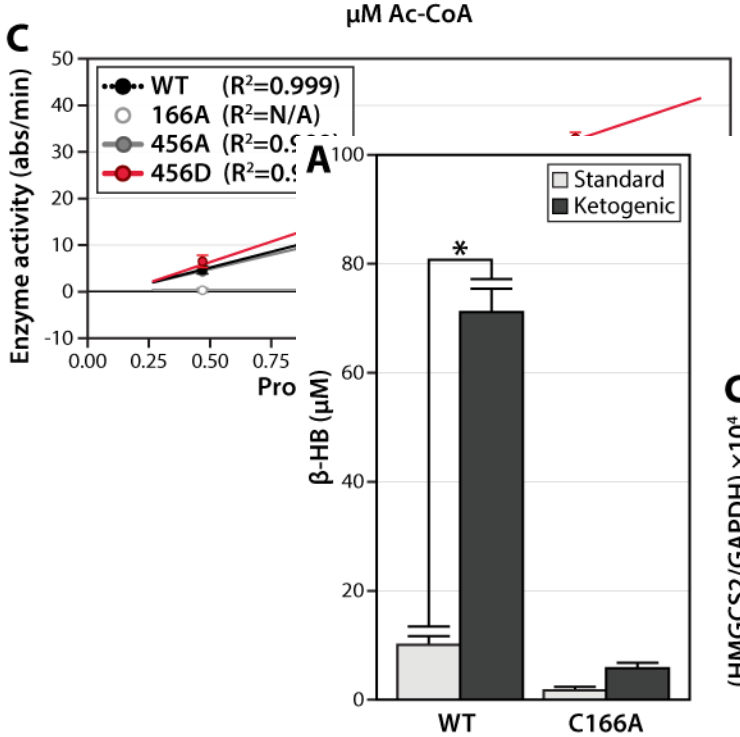

Figure S4. Additional information for screening candidate regulatory phosphosites on HMGCS2, Related to Figure 6. A) Upon sequencing the Hmgcs2 gene in B6 and BTBR mice, we confirmed that the BTBR strain harbor a coding SNP that causes a proline-to-threonine amino acid substitution at position 434 (codon change CCC to ACC). When the database used for searching the tandem MS spectra (from all mice in the multivariate study) is kept as the default UniProt sequence (*left*) or is manually altered to change Hmgcs2 residue 434 from P to T (*right*), the iTRAQ-based quantification of the non-phosphorylated peptide sequence spanning residues 433 and 434 is in agreement with strain difference in residue 434. While the different peptide sequences appear to have relatively equal abundance as estimated by spectral counts (64 vs. 62 PSMs for the non-phosphorylated sequences), the iTRAQ reporter intensity changes demonstrate how a coding SNP effects isobaric tag-based quantification of peptides spanning the effected residue. As such, although phosphorylation of serine 433 is unambiguously present in both mouse strains (21 PSMs in the context of the B6 sequence and 2 PSMs in the context of the BTBR sequence in the multivariate study), the relative abundances of this site cannot be measured using the iTRAQ system. We provide this as a cautionary reminder that such variants need to be considered in proteomic analyses seeking to compare organisms of different genetic backgrounds. B) Kinetic curve showing activity of wild type (WT), S433A, S433D, and S166A (catalytically dead) HMGCS2 at multiple concentrations of substrate. C) Enzyme activity at multiple concentrations of protein for FLAG-tagged wild type (WT), S456A, S456D, and C166A (catalytically dead) HMGCS2. Error bars indicate SD.

Figure S5. Expression of exogenous and lack of expression of endogenous HMGCS2 in HEK293 cells, Related to Figure 7. A) β-hydroxybutyrate (β-HB) levels were measured in culture medium from HEK293 cells transfected with WT or C166A HMGCS2, and subsequently cultured for 72 hours in either standard or ketogenic media. B) Immunoblot of the indicated FLAG-tagged Hmgcs2 variants (anti-FLAG antibody) and actin loading control (anti-β-actin antibody) in HEK293 cells transfected with pcDNA3.1 and cultured for 72 hours in either standard or ketogenic media (1 μg of protein from whole-cell extracted was loaded for each sample). C) RT-PCR analysis of endogenous HMGCS2 expression levels in positive control AML12 (mouse liver cell line) and HEK293 (derived from human embryonic kidney) cells used for the experiments in Figure 7. Values are expressed as mRNA levels (relative to control GAPDH) x 10,000. Error bars indicate SD and asterisks (*) indicate significance at $p<0.05$

Supplemental Tables

Tables S1-5. All protein and phosphoisoform quantitation for the univariate and multivariate experiments, Related to Figure 1. Measured species include protein abundance, phosphoisoform abundance (both with and without normalization to protein levels), phosphorylation motif abundance (both with and without normalization of underlying phosphoisoforms to protein levels), and predicted kinase activities (both with and without normalization of underlying phosphoisoforms to protein levels). Each file contains two tabs– the first tab contains a description and the second tab contains the data (note, Table S1 contains a third tab with information on all identified phosphopeptides). See Figure S1A for a visual depiction of comparisons made in each of the following files:

Table S1: Conditional Stats. Microsoft Excel file including condition-specific statistics for each proteomic/phosphoproteomic measurement (including phosphorylation motif and kinase activity predictions), such as mean (both $\log_2$ and geometric, relative to all eight conditions), standard deviation, and the number of replicate measurements (second tab). Also includes sequence coverage for each protein, and peptide spectral counts (PSMs), localized phosphopeptide sequences, and matching kinase preferences and motifs for all phosphoisoforms (note this information is only listed in Table S1 for brevity, but applies to the corresponding phosphoisoforms in Tables S2-5 as well). Also includes information on spectral quality for every localized and non-localized phosphopeptide identified at 1%FDR (note, only localized phosphopeptides were used for the analysis throughout this manuscript, but non-localized phosphopeptides can still provide valuable information regarding phosphorylation on proteins of interest, albeit without the assignment of the exact residue that is modified on the identified peptide at 95% probability).

Table S2: 1vs7. Microsoft Excel file including proteomic/phosphoproteomic comparisons (including phosphorylation motif and kinase activity predictions) between each physiological condition and the other seven, one at a time for all eight conditions.

Table S3: Factors. Microsoft Excel file including combinations of proteomic/phosphoproteomic comparisons (including phosphorylation motif and kinase activity predictions) between sets of physiological conditions linked by a common factor and all other conditions.

Table S4: 2vs2. Microsoft Excel file including combinations of proteomic/phosphoproteomic comparisons (including phosphorylation motif and kinase activity predictions) between a pair of two physiological conditions and another pair separated by a single variable.

Table S5: 1vs1. Microsoft Excel file including combinations of proteomic/phosphoproteomic comparisons (including phosphorylation motif and kinase activity predictions) between one physiological condition and another separated by a single variable.

Table S6. Protein abundance changes for selected pathways, Related to Figure 1. The underlying statistics (fold change, p-values, and q-values) for the pathway member protein abundance measurements highlighted in Figure 1G (OxPhos) and Figure S1G (Glycolysis and TCA cycle) are indicated on separate tabs (OxPhos on first tab, Glycolysis/TCA cycle on second tab) of a Microsoft Excel file (Note, these same measurements and additional comparisons for these proteins are also included in Tables S1-5).

Table S7. All protein and phosphoisoform quantitation for the fasting and refeeding experiment, Related to Figure 4. Measured species include protein abundance, phosphoisoform abundance (both with and without normalization to protein levels) for fasted and refed mice. The file contains three tabs– the first tab contains a description, the second tab contains the quantitative data, and the third tab contains information on all localized and non-localized phosphopeptides identified at 1% FDR (note, only localized phosphopeptides were used for the analysis throughout this manuscript, but non-localized phosphopeptides can still provide valuable information regarding phosphorylation on proteins of interest, albeit without the assignment of the exact residue that is modified on the identified peptide at 95% probability). Measurements include mean and standard deviation for each condition, relative to both conditions, and comparison statistics of $\log_2$ fold change (Fed/Fasted), fold change (Fed/Fasted), p-values, and q-values. Also includes sequence coverage for each protein and peptide spectral counts (PSMs) for each phosphoisoform.

SUPPLEMENTAL EXPERIMENTAL PROCEDURES

Chemicals and Supplies. 8-plex iTRAQ Reagents were purchased from Applied Biosystems (Carlsbad, CA). Protease (Complete mini EDTA-free) and phosphatase (PhosSTOP) inhibitor cocktail tablets were purchased from Roche (Mannheim, Germany). The BCA Protein Assay Kit was purchased from Pierce Biotechnology (Rockford, IL). Trypsin Gold, Protein Kinase A, and Caseine Kinase 2, were purchased from Promega (Madison, WI). Lysyl Endopeptidase (LysC) and Autokit Total Ketone Bodies were purchased from Wako Chemicals (Richmond, VA). Sep-Pak tC_{18} and C_{18} cartridges were purchased from Waters (Milford, MA). A Poly SULFOETHYL A column (200 x 9.4 mm, 5 mm, 200 Å) was purchased from PolyLC (Columbia, MD). Ni-NTA Magnetic Agarose Beads and Single-Tube Magnet were purchased from Qiagen (Valencia, CA). C_{18} resin (5 μm pore size) was purchased from Alltech (Deerfield, IL). Inline MicroFilters and MicroTight column unions, fittings, and sleeves were purchased from Upchurch Scientific (Oak Harbor, WA). Fused-silica capillary tubing was purchased from Polymicro Technologies (Phoenix, AZ). LITHISIL lithium silicate was purchased from PQ Corporation (Valley Forge, PA). Formic acid and trifluoroacetic acid ampoules were purchased from Thermo Scientific (Rockford, IL). Gibco Dulbecco's Modified Eagle Medium (DMEM), Fetal Bovine Serum (FBS), Phosphate Buffered Saline (PBS), Trypsin-EDTA, and Penicillin-Streptomycin were purchased from Life Technologies (Carlsbad, CA). Anti-FLAG M2 beads and FLAG peptide were purchased from Sigma. Mouse monoclonal anti-FLAG (HRP-linked) and anti-β-actin antibodies were purchased from sigma and anti-mouse IgG secondary antibody (HRP-linked) was purchased from Cell Signaling. All other chemicals were purchased from Sigma-Aldrich (St. Louis, MO).

Mitochondrial enrichment. Crude mitochondrial enrichment was performed using previously described methods (Pagliarini et al., 2008), modified for phosphoproteomics, with all steps carried out at 4ºC. Frozen (-80ºC) liver sections (~150 mg wet tissue weight) were placed into a Potter-Elvehjem glass/Teflon homogenizer along with 8 mL of MSHE Buffer (220 mM Mannitol, 70mM sucrose, 5mM HEPES, pH 7.4ImM EGTA, 1x protease inhibitor tablet, and 1x phosphatase inhibitor tablet) supplemented with 0.5% BSA. The tissue was homogenized with 4 homogenizer strokes at 1000 rpm, and the resulting homogenate was decanted into a new tube. The homogenizer was rinsed with an additional 2 mL MSHE (supplemented with 0.5% BSA), which was added to the homogenate. The sample was centrifuged at 800 x g for 10 min in a bench-top conical centrifuge. The small amount of lipid that formed at the top of supernatant was carefully aspirated. The supernatant, containing the mitochondria, was gently drawn off with a pipet-aid and transferred to an ultra-clear 12 mL centrifuge tube. The samples were centrifuged at 8000 x g for 10 min, and the resulting supernatant and any loose material was aspirated and discarded, leaving a dark brown pellet with a light brown halo around the center. An additional ImL of MSHE Buffer (supplemented with 0.5% BSA) was added to the pellet, which was disrupted by washing it from the side of the tube until homogenous using as few pipetting strokes as possible. Crude mitochondria were transferred to a 1.5 mL microfuge tube and centrifuged at 8,000 x g for 10 min in bench-top centrifuge. The supernatant was aspirated and discarded. The pellet was re-suspended in MSHE (without BSA) and centrifuged at 8,000 x g for 10 min in bench-top centrifuge. The supernatant was aspirated and discarded, and the mitochondrial pellet was flash frozen in liquid N_2 and stored at -80ºC until ready for use.

Protein digestion and iTRAQ labeling of peptides. Proteins were digested using modifications to previously described methods (Grimsrud et al., 2010). Crude mitochondrial pellets were re-suspended in 350 μl Resuspension Buffer (8M urea, 40 mM Tris, pH 8.0, 30 mM NaCl, ImM Na orthovanadate, 6 mM Na pyrophosphate, 2 mM $MgCl_2$, 1 mM $CaCl_2$, 1X protease inhibitor tablet, 1x phosphatase inhibitor tablet). Following mild heating at 37ºC for 1 hour with intermittent incubation in a sonicating water bath in three 10 minute intervals, protein concentration was determined using the BCA assay. After DTT was added to a final concentration of 2 mM, the samples were vortexed and incubated at 37ºC for 30 minutes to reduce disulfides. Samples were cooled to room temperature, iodoacetimide was added to a final concentration of 7 mM, and the samples were vortexed and incubated at room temperature in the dark for 30 minutes to alkylate cysteines. Additional DTT was added to a final concentration of 7 mM to quench the unreacted iodoacetimide. For each sample, 500 μg of protein was aliquoted to a new tube and enough Resuspension Buffer was added to bring the samples up to equal volumes. After addition of 5 μg LysC to each sample, the samples were vortexed and incubated at 37ºC for 4 hours. After the urea concentration was subsequently diluted to 1.5M by the addition of 50 mM Tris, pH 8.0, ImM $CaCl_2$, 5μg trypsin was added, and the samples were vortexed and incubated overnight at 37ºC. Enough 10% TFA was added (final concentration ~1%) to acidify the sample, and the peptides were desalted by solid phase extraction (SPE) using 50 mg tC_{18} Sep-Pak cartridges (Waters). Samples were dried in a speed vac, and labeled with 8-plex iTRAQ reagents. For all replicates, each sample was reconstituted in 20 μl dissolution buffer and 14 μl water, and mixed with the contents of one vial of a unique 8-plex iTRAQ reagents (tags 113 through 119, and 121), which had been previously dissolved in 50 μl isopropanol (see mitomod.biochem.wisc.edu for all iTRAQ tag-mouse pairings). The samples were incubated for 1 hour at room temperature, vortexing briefly every 15 minutes. For each replicate, 2μl of all eight samples was removed, combined, and subjected to a small-scale (no peptide pre-fractionation or phosphopeptide enrichment) LC-MS/MS test—utilizing beam-type collisional activation dissociation in the ion injection pathway (iHCD) of a modified linear ion trap (LTQ, Thermo Scientific) mass spectrometer (McAlister et al., 2011)—to test for complete iTRAQ labeling and equal sample mixing. The individual iTRAQ-labeled peptide samples were stored at -80ºC until further use.

Peptide fractionation and phosphopeptide enrichment. After confirming complete iTRAQ labeling, peptide samples were mixed in equal ratios (adjusting for any deviation from 1:1:1:1:1:1:1:1 in the small scale test mixture assessment described above) for each replicate separately, dried in a speed vac, and subjected to strong cation exchange (SCX) chromatography as described previously (Swaney et al., 2009), with slight modifications. Samples were re-suspended in 400 μl SCX Buffer A (5 mM KH_2PO_4, 30% acetonitrile, pH 2.65) and enough diluted phosphoric acid was added (~40 μl) to bring the pH below 3. Samples were injected on a polysulfoethylaspartamide column (9.4 x 200 mm; PolyLC) and a surveyor LC quaternary pump (Thermo Scientific) was

operated at a flow rate of 3.0 ml/min. Typically, 6 SCX fractions were collected over 36 minutes using the following gradient: 0-1 min, 100% SCX Buffer A; 0-2.5 min, 0-10% SCX Buffer B (5 mM KH_2PO_4, 30% acetonitrile, 350 mM KCl, pH 2.65); 2.5-17.5 min, 10-60% SCX Buffer B, 17.5-20.5 min, 60-100% Buffer B. Buffer B was held at 100% for 3.5 minutes. The column was washed for 4 min with SCX Buffer C (50 mM KH_2PO_4, 500 mM KCl, pH 7.5) followed by 2.5 min with water, prior to re-equilibration with SCX Buffer A. For one technical replicate of the univariate study (Figure 1A), however, 16 fractions were collected over a longer gradient, as used previously for whole cell analysis (Swaney et al., 2009). After it was determined that decreasing the number of fractions and shortening the gradient for a second technical replicate of the univariate study did not decrease the number of MitoCarta protein identifications, 6 SCX fractions and the above gradient were utilized for all of the biological replicates for the multivariate and fasting/refeeding studies. Fractions were frozen at -80ºC, lyophilized, desalted by SPE, and dried in a speed vac.

Each desalted SCX fraction was re-suspended in 1 ml 80% acetonitrile/0.1% TFA. For each sample, 5% (50 μl) was removed, dried in a speed vac, and saved at -80ºC for quantification of non-phosphopeptides. The remaining 95% (950 μl) of each fraction was subjected to immobilized metal affinity chromatography (IMAC) with magnetic beads (Qiagen) to enrich for phosphopeptides, as described previously (Phanstiel et al., 2011). Following three washes with water, the beads were incubated in 40 mM EDTA, pH 8.0 for 30 minutes while shaking, and subsequently washed with water again three times. The beads were then incubated with 100 mM $FeCl_3$ for 30 minutes while shaking, and were washed once with a 1:1:1 solution of acetonitrile/methanol, 0.1% acetic acid and three times with 80% acetonitrile/0.1% TFA. Samples were added to the beads and were incubated for 30 minutes while shaking, and subsequently washed four times with 1 ml 80% acetonitrile/0.1% TFA and eluted for 1 minute by vortexing in 100 μl of 1:1 acetonitrile:0.7% NH_4OH in water. Eluted phosphopeptides were acidified immediately with 5% formic acid and dried in a speed vac.

Nano-LC-MS/MS. High mass accuracy tandem MS was utilized for isobaric tag-based quantitative proteomics using our previously described methods (Lee et al., 2011; Phanstiel et al., 2011), with slight modifications. All samples were reconstituted in 20ul 0.2% formic acid. Precolumns (75 μm inner diameter x 5 cm) and analytical columns (50 μm inner diameter x 15 cm) were made in-house with C18 particles (Alltech), as described previously (Ficarro et al., 2009). For each Nano-LC-MS/MS run, a nanoACQUITY UPLC system (Waters Corporation) was used to load 4.5 μl of sample onto a precolumn for concentrating and desalting for 10 min at a flow rate of 1 μl per minute. Peptides were subsequently separated over an analytical column at a flow rate of 300 nL/min using gradients of varied amounts of LC Buffer A (0.2% formic acid) and LC Buffer B (100% acetonitrile, 0.2% formic acid). Phosphopeptide fractions were separated over the following gradient: 0-1 minute, hold at 1% acetonitrile; 1-115 minutes, 1–30% acetonitrile; 115-120 minutes, 30-80% acetonitrile; 120-125 minutes, isocratic elution at 80%. For non-phosphopeptide fractions, the following gradient was used: 0-1 minutes, 1–5% acetonitrile; 1-160 minutes, 5-25% acetonitrile; 160-180 minutes, 25-35% acetonitrile; 180-185 minutes, isocratic elution at 80% acetonitrile.

Eluted peptides were subjected to electrospray ionization (Fenn et al., 1989) and online infusion into an ETD-enabled LTQ Velos Orbitrap mass spectrometer (Thermo Fisher Scientific). MS^1 survey scans of peptide cations were performed in the orbitrap at 30,000 or 60,000 resolution, precursors were selected for fragmentation using a 3.0 Th isolation window, and orbitrap MS/MS interrogation was performed at 7,500 resolution. At least two runs were performed for each sample where the top ten most abundant ions of charge state 2 or greater from each MS^1 scan were selected for fragmentation with HCD (45 normalized collision energy). An additional run using back-to-back ETD (35 normalized collision energy, 70 ms activation time) and HCD on the top five most abundant precursors of charge state 3 or greater was performed on each phosphopeptide fraction. Dynamic exclusion was enabled for 60 s, with a max exclusion list of 500 with an exclusion width of 0.55 Th below and 2.55 Th above the selected average mass. MS/MS was always performed in the LTQ. Tune methods had AGC target settings of $1x10^6$ for $FTMS^1$, $5x10^4$ for $FTMS^N$, and $4x10^5$ for ETD reagent ions, and max inject times of 200 ms for $FTMS^1$, 200 ms for FT MS^N, and 100ms for ETD. For all runs from the multivariate study, real-time precursor purity filtering (RTF) was performed on the fly during precursor selection by modification of the instrument control method as described previously (Wenger et al., 2011a). Using RTF, precursors were only selected for fragmentation if they had interfering ions present below a threshold of 0.25 times the precursor's intensity within an m/z window of 3.6 Th. For the univariate study, post-acquisition filtering (PAF) was applied to remove quantitation for MS^2 spectra with this same level of interference (0.25) observed in their corresponding MS^1 spectrum, as described previously (Phanstiel et al., 2011). For the fasting/refeeding study, peptide and phosphopeptide fractions from each of 6 SCX fractions were subjected to two runs: one run used all HCD fragmentation (35 normalized collision energy) (applying PAF as described above, dynamic exclusion of 10 ppm around selected isotopes, MS1 AGC of $1x10^5$, and max inject time of 100 ms) and one run used HCD fragmentation (40 normalized collision energy) along with our recently developed instrument control method, QuantMode, which increases quantitative accuracy and dynamic range for isobaric-labeled samples through gas phase purification of peptides prior to dissociation (Wenger et al., 2011a). SF_6 reagent ions were used to perform the proton transfer reaction required to purify precursors. MS2 AGC and max inject times were set to $2x10^6$ and 200 ms respectively.

Sequence identification and protein/phosphoprotein quantitation. The Coon OMSSA Proteomics Software Suite (COMPASS) was utilized to analyze tandem MS spectra as described previously (Wenger et al., 2011b). Merged .dta text files consisting of MS^2 peak lists were extracted from Thermo .raw files were generated using the COMPASS module *DTA Generator*. Remaining precursors were removed from all spectra and ETD preprocessing was performed for ETD spectra, which increases database search identifications (Good et al., 2009). The Open Mass Spectrometry Search Algorithm (OMSSA) (Geer et al., 2004) was used to search peak lists against a concatenated target-decoy database (Elias and Gygi, 2007) consisting of mouse proteins are their nonsense reverse complements. The *Mus musculus* complete proteome set, consisting of reviewed (UniProtKB/Swiss-Prot) and unreviewed (UniProtKB/TrEMBL) protein sequences from UniProt (www.uniprot.org/taxonomy/10090) was utilized as the target protein database, which contained 48,070 entries at the

time of download (8/3/11). The decoy entries for concatenated target-decoy database were prepared with *Database Maker* by reversing the protein sequences for all UniProt entries. All database searches included a precursor mass tolerance setting of ±4.5 Da and monoisotopic mass tolerance of ±0.01 Da for fragment ions, and allowed for up to 3 missed cleavages with trypsin. Fixed modifications included carbamidomethylation of cysteines and 8-plex iTRAQ (as a user modification) on the N-terminus and lysines. Standard variable modifications included oxidation of methionines and 8-plex iTRAQ on tryosines. For phosphopeptide runs specifically, additional variable modifications included phosphorylation with neutral loss on serine and threonine residues and intact phosphorylation on tyrosine residues for HCD spectra, and intact phosphorylation on serine, threonine, and tyrosine for ETD spectra. For each replicate, identifications from non-phosphopeptide and phosphopeptide runs were separately filtered to an estimated 1% false discovery rate (FDR) at the unique peptide level with *FDR Optimizer*. The COMPASS module *TagQuant* was utilized to assign quantitative values to all peptide spectral matches (PSMs) using iTRAQ reporter ion intensities, apply isotope purity corrections, and normalize quantitation for all PSMs across each replicate individually (with data from corresponding phosphopeptide runs and non-phosphopeptide runs normalized together) as a loading control. *Protein Hoarder* was used to group peptides (from all replicates together) to parsimonious protein groups at 1% FDR at the unique protein level (using only peptides unique to each protein group for protein-level scoring), and sum the reporter ion intensities of all PSMs (with interference below 0.25, as described above) for a given unique protein within each replicate individually. Phosphopeptides and peptides shared between protein groups were excluded from protein quantitation calculations. *Phosphinator* was utilized to localize phosphoryl groups to specific residues at 95% probability (Ascore = 13) (Beausoleil et al., 2006)for all phosphopeptides identified at 1% peptide level FDR and sum reporter ion intensities of all localized phosphopeptides identifying a given phosphoisoform (pattern of co-detected localized phosphorylation sites) within each replicate individually (Phanstiel et al., 2011).

Statistical comparisons of proteomic measurements. We converted the .csv files from *Protein Hoarder* and *Phosphinator* to a tab-delimited format and reduced the protein descriptions to UniProt protein names. An in-house program written in Microsoft Access, called *COMPASS Reader*, processed the data in an automated fashion. The processing is stored in Access tables and then converted to Excel workbooks for ease of use. *COMPASS Reader* utilized the following workflow:

1) ***Import***– Import to normalized database structure. All data is imported into a set of tables. This transformation includes, for example, the separation of data values (measurements) from metadata (e.g. names of proteins).
2) ***Value Transformation***– Truncated Log Transform. Individual values are converted into a form that approximates a normal distribution overall. In our case we needed to discard all measurements less than 2^{12} and take the log (base 2) of the remaining measurements.
3) ***Value Normalization***– Removal of Block Effect. For each measurement-replicate we compute the average across all measured samples and reduce the condition-measurement-replicate by the mean. Note that this step is only relevant for display of the measurements for all eight physiological conditions; the various comparisons between sets of conditions automatically remove this block effect.
4) ***Reduce technical replicates***– Average measurements from the same mouse. This reduces the two technical replicates of the univariate experiment to a single collection of 8 mice, but has no effect on the multivariate experiment.
5) ***Score Protein Significance***– *t*-test. For each measurement-comparison (see below for list of comparisons), compute a p-value for the null hypothesis that the In-Group has the same (normal) distribution as the Out-Group. We assume the same variance for this test.
6) ***Multiple Hypothesis Testing***– FDR Calculation. For each measurement_type-comparison we count the number of measurement comparisons that have a p-value greater than 0.5. We use this as an estimate of half of the True Negative cases (TN) (i.e. measurements that do not change between the two groups of the comparison). We assume that the p-values of unchanging measurement-comparisons are uniformly distributed between 0 and 1 (Figure S1E); this means that the expected number of false positives with p-values less than x is equal to x times TN. Thus, we can count the number of estimated positives (Pos(x)) who have p-values less than x. This gives us an estimate of the FDR as: FDR(x) = x * TN / Pos(x). Finally we force our FDR estimate to be non-decreasing (x<y implies that FDR(x)≤FDR(y)). Note that this method produces both an estimate of the number of true positives (i.e. measurements that are changing between two collections of conditions) and an FDR that is usually less than 100% for p=1.0. This FDR calculation was applied to protein, phosphoisoform, and normalized phosphoisoform measurements (but not motif or kinase activity predictions due to the smaller number of measurements).
7) ***Relevance Filter***– *q*-value cutoff. Select an arbitrary cut-off for the FDR. Note that a *q*-value (FDR) is an estimate of the probability that the alternate hypothesis is incorrect, which is a different type of object from the traditional *p*-value. While $p<0.05$ is a traditional cutoff in much of biology (which, in principle, means that 5% of conclusions based on random noise are considered real), the cutoff for a *q*-value should be evaluated based on the researcher's tolerance of an incorrect answer; we have chosen to highlight changes at $q<0.1$ in this manuscript, which assumes that 10% of the changes deemed significant are wrong, which is a common cutoff used in transcriptomics (Zheng et al., 2010). However, other researches can utilize either more or less conservative q-value thresholds when utilizing our data.

Description of Proteomic Comparisons. We produced two types of comparisons: *conditional* and *restricted*. The *conditional* comparisons compare a subset of the conditions with the remainder of the conditions. Examples:

- **BTBR**: Compares BTBR mice with B6 mice. This is the strain comparison.
- **BTBR_O**: Compares BTBR/obese mice with all others (all B6 mice and all lean mice)
- **BTBR_O_10**: Compares BTBR/obese/10 week mice with all other mice. This comparison is also called Diabetes since it is the only condition

where the diabetic phenotype exhibits.

We performed 8 single-condition comparisons (corresponding to the eight unique conditions), 3 two-condition comparisons (BTBR_O, BTBR_10, O_10), and 3 four-condition comparisons (BTBR, Obese, and 10 weeks), for a total 14 comparisons. For emphasis, the diabetic state is represented twice (as stated above), once as BTBR_O_10 and once as Diabetes, bringing the nominal number of comparisons to 15. We refer to single-condition comparisons as the "Iv7 comparisons" (Table S2) and the rest as the "Factor comparisons" (Table S3). The rest of the comparisons, the "*restricted* comparisons", compare differences for a single factor (e.g. obesity) for a restricted set. Examples:

- **Obesity-BTBR**: Compares all obese/BTBR mice with all lean/BTBR mice
- **Obesity-B6_04**: Compares all B6_O_04 mice with all B6_L_04 mice

There are 3 factors to compare (Obesity (obese vs lean), Strain (BTBR vs B6), and Age (10 weeks vs 4 weeks)). For each factor, there are 4 single-factor restrictions and 4 double-factor restrictions, for a total of 24 comparisons. Thus, the total number of comparisons is 38, with 1 duplicate labeling of the same comparison (BTBR_O_10, a *Iv7* comparison, is the same as Diabetes, a *factor* comparison). These comparisons are separated into four Microsoft Excel files (Tables S2-5, see Figure S1A for a visual key of comparisons and in which files they are found).

We also created a file referred to as Conditional Stats (Table S1). This includes mean, variance, standard deviation, and count of all measurement-conditions. Conditional Stats is related to the Iv7 comparison but still contains unique information, as it does not compare information across the conditions (beyond the data normalization, which forces the mean of all conditions to be zero). The $\log_2$ mean presented in Conditional Stats and the $\log_2$ fold-change presented in Iv7 differ by $1/7^{th}$, since the Iv7 subtracts the mean for 7 conditions from the mean of 1 condition (which will be of opposite sign) whereas the Conditional Stats only uses the mean. The Conditional Stats file is ideal for obtaining values for graphical representation of each measurement (with standard deviations), where the comparison files (Tables S2-5) should be utilized for evaluating magnitude and statistical significance of changes between conditions. This file also includes information about sequence coverage and spectral counts for estimating absolute abundance rank, and phosphopeptide sequences used for identifying phosphorylation sites on UniProt proteins.

Kinase-substrate predictions. Motifs were calculated using Motif-X v1.2 (Schwartz and Gygi, 2005), using a motif width of 35, a minimum occurrence threshold of 20, and a significance threshold of 0.000001. Motif analysis was run separately for analysis of serine, threonine, and tyrosine phosphorylation. For analysis of phosphorylation motifs present in our entire dataset, all localized phosphopeptides were utilized as the input with the IPI mouse proteome as the background. For analysis of mitochondrial-specific phosphorylation motifs, only localized phosphopeptides mapping to MitoCarta proteins were utilized as the input and sequences from the mouse MitoCarta list at http://www.broadinstitute.org/ftp/distribution/metabolic/papers/Pagliarini/Mouse.MitoCarta.fasta (Pagliarini et al., 2008) were uploaded as the background. Kinase preferences were taken from the PHOSIDA database at http://141.61.102.18/phosida/help/motifs.aspx (Gnad et al., 2011).

HMGCS2 purification. Cells were lysed on ice in IP buffer (PBS with 0.5% NP-40) supplemented with protease (Complete, Roche) and phosphatase (PhosSTOP, Roche) inhibitor cocktail tablets added just before use. Cells were sonicated at 20% output for 15 seconds and spun at 8,000 x g to clarify the lysate. FLAG-tagged proteins were immunoprecipitated using anti-FLAG M2 beads (Sigma) overnight at 4°C and washed five times with 10mL of IP buffer. For HMGCS2 activity assays, immunoprecipitated HMGCS2-FLAG proteins were eluted with 0.25mg/mL FLAG peptide (Sigma), concentrated using a centrifugal filter unit with 10kDa pore size (Millipore) and buffer exchanged with PBS / 15% glycerol / 0.1mM DTT as described previously (Shimazu et al., 2010).

Synthesis and extraction of Acetyl-Coenzyme A. Acetyl Coenzyme A was synthesized as previously described (Parthasarathy et al., 2011; Stadtman, 1957), with slight modifications. Acetic anhydride and 0.5 M sodium bicarbonate were cooled on ice, and the free Coenzyme A was dissolved into the sodium bicarbonate in a round-bottom flask. The reaction flask was cooled on ice, and acetonitrile was added to 10% (v/v). Acetic anhydride was then added in a 1.5:1 molar ratio to the Coenzyme A and the reaction was allowed to proceed for 15 minutes on ice. After spotting the reaction onto Whatman paper, reaction completion was monitored by staining with nitroprusside and observing a color change after addition of methanolic sodium hydroxide. After a 15 minute reaction in a round bottom flask, the solution was acidified to a pH of ~ 2 with 6N HCl and frozen in liquid N_2 before lyophilizing overnight. To isolate acetyl Coenzyme A from the reaction, C_{18} Sep-Pak columns (Waters) were pre-washed with methanol and equilibrated with 0.1% TFA. The acetyl Coenzyme A reaction solid was removed from the lyophilizer, placed immediately on ice, and subsequently dissolved in 0.1% TFA. The AcCoA solution was then loaded onto the Sep-Pak column and washed with 0.1% TFA. After washing, acetyl Coenzyme A was eluted using into 3 asymmetric fractions using 4 mL of 0.1% TFA/CAN (1:1). Fraction 1 contained 0.5 mL and was discarded, fraction 2 contained 2 mL and was reserved, and fraction 3 contained 1.5 mL and was also discarded. Fraction 2 was then frozen in liquid N_2, lyophilized overnight, and the weight of the subsequent Acetyl-CoA was used to calculate reaction yield.

HMCSC2 activity assay. HMGCS2 enzymatic activity was measured as described previously (Shimazu et al., 2010; Skaff and Miziorko, 2010). Briefly, activity was measured by monitoring the formation of HMG-CoA by Ac-CoA and AcAc-CoA, as measured by DTNB detection of CoASH (Skaff and Miziorko, 2010). Ac-CoA was synthesized based on previously described methods (Parthasarathy et al., 2011; Stadtman, 1957). Assay mixtures contained 10 μM AcAc-CoA and 0-

2000uM Ac-CoA. Standard assay conditions used 1 µg of FLAG-HMGCS2 protein. Absorbance at 412 nm was recorded and data reflecting linear rates was collected for all enzymes. Using non-linear regression (Prism), data was fitted to the Michaelis-Menten equation to determine Km and Vmax for each mutant. A unit of enzyme activity is defined as the amount of enzyme required to convert 1 µmol of substrate into product in one minute.

***In vitro* kinase assay.** Purified HMGCS2 protein (1-2 µg) was incubated with or without 5U of cAMP dependent protein kinase catalytic subunit (PKA, Promega) or 2U of Casein Kinase 2 (CK2, Promega). Incubation was performed in kinase reaction buffer (BSA, Tris, ATP) for 30min at 30°C. After incubation, enzyme activity was assayed as described above using 750 uM of Acetyl CoA as a substrate.

Ketone body measurement. Ketone body levels were measured following the manufacturers protocol using the Autokit Total Ketone Bodies assay (Wako). Briefly, known standards of β-hydroxybutyrate and unknown sample were loaded onto a 96-well plate (Fisher). After incubation with R1 buffer containing Thio-NAD for 5 min at RT, R2 buffer was added to the samples and the production of Thio-NADH was monitored at 405 nm for 15 min using a BioTek Synergy 2 microplate reader. The rate of the reaction at different KB concentrations was used to create a standard curve and calculate the concentration of ketone bodies in the experimental samples.

Quantiative RT-PCR. RNA was isolated from HEK293 or AML12 cells using an RNeasy kit (Qiagen) according to manufacturer's instructions. Exon-spanning primers were designed for human HMGCS2 (accession# NM_005518) and GAPDH or murine Hmgcs2 (accession# NM_008256) and Gapdh to detect expression in 293 and AML12 cells, respectively. Primer sequences used are: human HMGCS2 (fwd: 5' TCCCTTTACCTCTCCACTCAC 3', rev: 5' CCATAAGAGAAGGCACCAATCC 3'), human GAPDH (fwd: 5' TTCGCTCTCTGCTCCTCCTGTT 3', rev: 5' GCCCAATACGACCAAATCCGTTGA 3'), mouse Hmgcs2 (fwd: 5' CATCGAGGGCATAGATACCAC 3', rev: 5' CACTCGGGTAGACTGCAATG 3'), and mouse Gapdh (fwd: 5' GCCTTCCGTGTTCCTACC 3', rev: 5' CCTCAGTGTAGCCCAAGATG 3'). RT-PCR was performed using Power SYBR Green PCR Master Mix (Invitrogen) and data was collected on an ABI-7500 Fast Real Time PCR System (Applied Biosystems). The comparative CT method was used to calculate relative Hmgcs2 or HMGCS2 expression levels.

SUPPLEMENTAL REFERENCES

Beausoleil, S.A., Villen, J., Gerber, S.A., Rush, J., and Gygi, S.P. (2006). A probability-based approach for high-throughput protein phosphorylation analysis and site localization. Nat Biotechnol *24*, 1285-1292.

Elias, J.E., and Gygi, S.P. (2007). Target-decoy search strategy for increased confidence in large-scale protein identifications by mass spectrometry. Nat Methods *4*, 207-214.

Fenn, J.B., Mann, M., Meng, C.K., Wong, S.F., and Whitehouse, C.M. (1989). Electrospray ionization for mass spectrometry of large biomolecules. Science *246*, 64-71.

Ficarro, S.B., Zhang, Y., Lu, Y., Moghimi, A.R., Askenazi, M., Hyatt, E., Smith, E.D., Boyer, L., Schlaeger, T.M., Luckey, C.J., et al. (2009). Improved electrospray ionization efficiency compensates for diminished chromatographic resolution and enables proteomics analysis of tyrosine signaling in embryonic stem cells. Anal Chem *81*, 3440-3447.

Geer, L.Y., Markey, S.P., Kowalak, J.A., Wagner, L., Xu, M., Maynard, D.M., Yang, X., Shi, W., and Bryant, S.H. (2004). Open mass spectrometry search algorithm. J Proteome Res *3*, 958-964.

Gnad, F., Gunawardena, J., and Mann, M. (2011). PHOSIDA 2011: the posttranslational modification database. Nucleic Acids Res *39*, D253-260.

Good, D.M., Wenger, C.D., McAlister, G.C., Bai, D.L., Hunt, D.F., and Coon, J.J. (2009). Post-Acquisition ETD Spectral Processing for Increased Peptide Identifications. J Am Soc Mass Spectrom.

Grimsrud, P.A., den Os, D., Wenger, C.D., Swaney, D.L., Schwartz, D., Sussman, M.R., Ane, J.M., and Coon, J.J. (2010). Large-Scale Phosphoprotein Analysis in Medicago truncatula Roots Provides Insight into in Vivo Kinase Activity in Legumes. Plant Physiol *152*, 19-28.

Lee, M.V., Topper, S.E., Hubler, S.L., Hose, J., Wenger, C.D., Coon, J.J., and Gasch, A.P. (2011). A dynamic model of proteome changes reveals new roles for transcript alteration in yeast. Mol Syst Biol *7*, 514.

McAlister, G.C., Phanstiel, D.H., Brumbaugh, J., Westphall, M.S., and Coon, J.J. (2011). Higher-energy Collision-activated Dissociation Without a Dedicated Collision Cell. Molecular & Cellular Proteomics *10*.

Pagliarini, D.J., Calvo, S.E., Chang, B., Sheth, S.A., Vafai, S.B., Ong, S.E., Walford, G.A., Sugiana, C., Boneh, A., Chen, W.K., et al. (2008). A mitochondrial protein compendium elucidates complex I disease biology. Cell *134*, 112-123.

Parthasarathy, A., Pierik, A.J., Kahnt, J., Zelder, O., and Buckel, W. (2011). Substrate specificity of 2-hydroxyglutaryl-CoA dehydratase from Clostridium symbiosum: toward a bio-based production of adipic acid. Biochemistry *50*, 3540-3550.

Phanstiel, D.H., Brumbaugh, J., Wenger, C.D., Tian, S., Probasco, M.D., Bailey, D.J., Swaney, D.L., Tervo, M.A., Bolin, J.M., Ruotti, V., et al. (2011). Proteomic and phosphoproteomic comparison of human ES and iPS cells. Nat Methods *8*, 821-827.

Schwartz, D., and Gygi, S.P. (2005). An iterative statistical approach to the identification of protein phosphorylation motifs from large-scale data sets. Nat Biotechnol *23*, 1391-1398.

Shimazu, T., Hirschey, M.D., Hua, L., Dittenhafer-Reed, K.E., Schwer, B., Lombard, D.B., Li, Y., Bunkenborg, J., Alt, F.W., Denu, J.M., et al. (2010). SIRT3 deacetylates mitochondrial 3-hydroxy-3-methylglutaryl CoA synthase 2 and regulates ketone body production. Cell metabolism *12*, 654-661.

Skaff, D.A., and Miziorko, H.M. (2010). A visible wavelength spectrophotometric assay suitable for high-throughput screening of 3-hydroxy-3-methylglutaryl-CoA synthase. Anal Biochem *396*, 96-102.

Stadtman, E.R. (1957). Preparation and Assay of Acyl Coenzyme A and Other Thiol Esters; Use of Hydroxylamine. Methods in Enzymology *3*, 931-941.

Swaney, D.L., Wenger, C.D., Thomson, J.A., and Coon, J.J. (2009). Human embryonic stem cell phosphoproteome revealed by electron transfer dissociation tandem mass spectrometry. Proc Natl Acad Sci U S A *106*, 995-1000.

Wenger, C.D., Lee, M.V., Hebert, A.S., McAlister, G.C., Phanstiel, D.H., Westphall, M.S., and Coon, J.J. (2011a). Gas-phase purification enables accurate, multiplexed proteome quantification with isobaric tagging. Nat Methods *8*, 933-935.

Wenger, C.D., Phanstiel, D.H., Lee, M.V., Bailey, D.J., and Coon, J.J. (2011b). COMPASS: a suite of pre- and post-search proteomics software tools for OMSSA. Proteomics *11*, 1064-1074.

Zheng, D., Kille, P., Feeney, G.P., Cunningham, P., Handy, R.D., and Hogstrand, C. (2010). Dynamic transcriptomic profiles of zebrafish gills in response to zinc supplementation. BMC Genomics *11*, 553.